

PROCESS SIMULATION OF ALUMINUM REDUCTION CELLS

Imad Tabsh, COMPUSIM Inc.

1003 D 55 Avenue N.E., Calgary, Alberta, Canada T2E 6W1

Marc Dupuis, GéniSim

3111 Alger, Jonquière, Québec, Canada G7S 2M9

Alexandre Gomes, Alcan Alumínio do Brasil S.A.

Cx. Postal 7391, Pituba, 41810-000 Salvador, BA, Brasil

Abstract

A program was developed to model the dynamic behavior of an aluminum reduction cell. The program simulates the physical process by solving the heat and mass balance equations that characterize the behavior of eleven chemical species in the system. It also models operational events (such as metal tapping, anode change, etc.) and the process control logic including various alumina feeding policies and anode effect quenching. The program is a PC based Windows[®] application that takes full advantage of the Windows user interface.

This paper describes the implementation of the process model and the control logic. Various results using the simulation are compared to measured data.

Introduction

The design and operation of an aluminum reduction cell is a complex task requiring a detailed understanding of the behavior of the cell. Several articles and papers have been written that describe the chemical process itself and the control logic used in operating cells. The information was used in the development of a PC based computer program that models the dynamic behavior of the cell.

Such a program would be valuable for developing more insight into the behavior of cells. The information can be used to improve cell performance and design new cells as well as retrofit existing ones. It can also be used for training pot operators and evaluating alternative control strategies.

This paper describes the minimum requirements needed to simulate the process as implemented in the program. Furthermore, it presents a comparison of the behavior predicted by the program with measurements from an operating cell. It concludes by presenting the impact of changing the feeding strategy on cell performance.

Program Overview

A mathematical model of the dynamic behavior of a reduction cell must represent the electrolysis process itself as well as the operating procedures used in the smelter. The task can be split into two main parts: a *Process Model* which simulates the physical process that characterizes the pot behavior; and a *Control Model* which simulates the pot operation as characterized by the operating procedures and the cell control algorithms.

The constitutive equations solved are obtained by evaluating the heat balance equation and mass balance equations of eleven chemical species over the system of interest. That system is defined as the liquid zone (bath and metal) and the solidified bath ledge. An additional differential equation is used to compute the dynamic evolution of the ACD for a total of 13 differential equations solved.

The state of the system at any point in time is defined by the 16 dynamic variables listed in Table I. The first 13 are calculated using the heat and mass balance equations while the beam position and cell state are evaluated as part of the control model. These variables along with TIME provide enough information to compute the evolution of the system.

Table I: List of Dynamic Variables

Anode to cathode distance (ACD)
Bath and metal temperature
Mass of bath
Mass of dispersed alumina
Mass of dissolved alumina
Mass of excess aluminum fluoride
Mass of calcium fluoride
Mass of lithium fluoride
Mass of magnesium fluoride
Mass of metal
Mass of sludge
Average thickness of freeze adjacent to bath
Average thickness of freeze adjacent to metal

Anode beam position
Cell state

Time

There are more than forty additional variables derived from the above and used to calculate the new state of the system:

The program is a Windows[®] application developed using the C++ object oriented programming language. It takes full advantage of the Windows environment to create a friendly and efficient user interface. Drop menus and dialogs are used to enter the model data. Time history plots are available to review the response of all variables in the simulation.

Process Model

Heat Balance Equations

The thermal balance of the system is obtained by evaluating the internal heat generation and the heat loss from the system. The difference represents the heat accumulated in the system.

The *internal heat* is evaluated by computing the voltage break down. The task is performed in modules each of which solves for a component of the voltage breakdown using submodels. A submodel consists of one or more equations that define the variable(s) in a module. The program has built-in equations for each submodel based on published data in the literature [1-7]. In addition, the user can customize the equations of a submodel using the internal variables available in the simulation.

The modules that define the internal heat are:

- Bath composition
- Bath resistivity
- Bath liquidus
- Current efficiency
- Bath voltage
- Electrolysis voltage
- Equivalent voltage to make metal

Evaluation of the *heat loss* is simplified by assuming that the heat produced in the system can escape from four different surfaces: the anode panel, the cathode panel, the ledge adjacent to the bath layer and the ledge adjacent to the metal layer.

A constant thermal resistance is assumed for the cathode and anode panels. Thus, the heat loss from these two surfaces is only a function of the difference between the operating temperature and the ambient temperature in the potroom. The anode panel includes everything above the top surface of the bath while the cathode panel includes everything below the bottom surface of the metal pad.

The thermal resistance adjacent to the ledge is a function of the average ledge thickness, the resistance of the mix and side carbon, and the convection from the potshell surface. The resistance changes continuously as the ledge melts and forms.

The difference between the internal heat and the global heat loss must accumulate in the system. There are two ways to accumulate heat in the system: melting/forming ledge and increasing/decreasing the operating temperature.

The problem of defining the melting rate of the ledge profile is referred to as the "Stefan problem". If the energy required to bring the melting ledge to the liquidus temperature is neglected, the melting rate and the corresponding equivalent heat flux can be easily evaluated [8]. In short, the heat flux equivalent to the freezing rate is characterized by the difference between the heat flux going into and out of the ledge. The former is a function of the local heat transfer coefficient at the surface of the ledge and the cell superheat. The latter is a function of the thermal resistance adjacent to the ledge and the global temperature gradient between the operating temperature and the ambient air temperature.

The remaining excess heat accumulates in the bath and metal as latent heat thus increasing or decreasing the operating temperature. A very high heat transfer coefficient is assumed at the bath/metal interface which, for all practical purposes, results in the same temperature for both. Note that the temperature is also affected by the latent heat and heat of dissolution of the alumina being fed and by the addition of bath and bath constituents.

One can see that there is a strong coupling between these two parallel mechanisms of heat accumulation. Increasing the operating temperature will increase the superheat that will in turn increase the freezing rate. Hence, one should not try to dissociate the two effects but should keep in mind that the key player is the cell superheat.

Mass Balance Equations

Eleven chemical species are considered in the mass balance equations:

- Metal.
- Bath which is a solution of cryolite, excess AlF_3 , dissolved alumina, CaF_2 , MgF_2 and LiF .
- Ledge adjacent to the bath layer.
- Ledge adjacent to the metal layer.
- Alumina dispersed in the bath.
- Sludge in the metal.

The *metal* mass balance is quite simple. The metal production rate is established from the instantaneous cell amperage and current efficiency. Metal is tapped out based on a user defined policy.

The *bath* mass balance is more involved. The mass of the bath and the concentration of the bath additives are computed by solving the mass balance of the six bath constituents:

- The *cryolite* mass balance is controlled by the formation of ledge and of sludge. Ledge is assumed to be a mixture of cryolite and alumina at the eutectic concentration. Sludge is assumed to be a mixture of cryolite and alumina at a concentration specified by the user.
- The mass of *excess AlF_3* is controlled by the fluoride evaporation submodel [9], the alumina feeding policy (if there is fluoride in the alumina feed), and by direct feeding using events defined by the user.
- The mass of *dissolved alumina* is controlled by the metal production rate and the alumina dissolution submodel [10]. There are three suppliers of alumina in the submodel implemented in the program: the alumina dispersed in the bath, the sludge present in the metal, and the ledge.
- The mass of *CaF_2 , MgF_2 and LiF* , if present, is controlled using events defined by the user.

The mass of *alumina dispersed* in the bath is controlled by the alumina dissolution rate and the sludge formation rate as well as the alumina feeding control submodel.

The mass of *sludge* is controlled by the sludge formation rate and the sludge back feeding rate.

The rate of change of the *thickness of the ledge* adjacent to the bath and to the metal is determined by the solution of the "Stefan" problem.

Note that bath transfusion events (adding and tapping bath) and the ratio adjustment events are also accounted for in the mass balance calculations.

Evolution of the ACD

The rate of change of the *ACD* is computed from the metal production rate, the sludge production rate, the rate of change of the thickness of the ledge adjacent to the metal, and the anode consumption rate. The *ACD* itself is also a function of the anode beam motion which is defined in the control model.

The *anode beam position* is continuously updated during the simulation. It is a function of all beam motions as well as the beam raising scheduled event. Anode adjustment initiated by the control model is prevented during the anode change and beam raising events.

Control Model

The behavior of the system is further influenced by the operational procedures of the smelter and the control logic implemented in the cell controller. They define the control model and are represented in the program as events and cell states.

The program provides for three categories of events: *operational*, *scheduled* and *exception*. Depending on the event, the start time and duration can be pre-set by the user or it can be determined by the program from the cell behavior. Furthermore, events are *continuous periodic* or *discrete*. Continuous events are characterized by a *rate* while periodic events are characterized by an *amount*, *frequency*, *duration* and *start time*. Discrete events are characterized by "Instances" consisting of the *time* when the action takes place, a *quantity* particular to the action and the *duration* of the action. Multiple instances can be associated with the event.

Operational Events

Operational events are ongoing actions that are part of the cell operation. They include *Alumina Feeding* and *Resistance Control*.

Alumina feeding depends on the cell technology. Point breaker feeder cells are operated in a "quasi-continuous" feeding mode. They can have the capability of automatically increasing and decreasing the feed rate by monitoring the cell resistance. Side break cells are operated in a "batch" feeding mode. Both feeding strategies are incorporated in the program.

Resistance control is characterized by the target resistance, the dead band, the back EMF voltage for calculating the pseudo resistance of the cell, and the distance the anode is moved.

The nominal feeding rate is adjusted during the simulation in accordance with the alumina feeding and the anode effect quenching control policies. The anode motion and/or the adjustment of the feeding rate is triggered by the control logic associated with the cell states.

Scheduled Events

These are pre-planned actions that take place at specified times. They include:

- *Metal Tapping* Removing metal from the pot.
- *Anode Change* Replacing spent anodes in a prebake cell.
- *Anode Beam Raising* Raising the anode beam to the top position.
- *Ratio Adjustment* Adding bath constituents to adjust the bath ratio.
- *Bath Transfusion* Adding or removing bath from the pot.

Scheduled events can be either unconditional or conditional. An unconditional *scheduled event* will always take place at the start time defined by the user provided that the start time is within the current simulation time span. The start time of *conditional scheduled events* is determined by the program based on predefined rules. Hence, the event may or may not take place depending on the condition of the cell.

Exception Events

These are events that are triggered as a result of the conditions within the pot such as anode effects or cell instability. Only the anode effect is implemented.

Cell States

There are five cell states implemented in the program: *normal*, *metal tapping*, *anode change*, *beam raising* and *anode effect*. Each state has an operational procedure or "control logic" Several procedures are pre-programmed which can be customized by defining the data that represent the particular cell. Cell states are mutually exclusive, hence the pot can be in only one state at a particular time. Switching between states is determined by the starting and ending time of events. Some events can occur in more than one cell state.

The various cell states deal with different events as the name suggests. Of particular importance is the *Normal* state where the aim of the cell controller is to maintain the dissolved alumina and ACD at their optimum levels as well as initiate the processing of scheduled and exception events. Typically, the cell will be in this state for more than 85% of the time.

Four models for the alumina feeding policy and ACD control are built into the program with options to customize the control variables. These include:

- *Constant Rate*: constant alumina feeding rate with standard resistance control.
- *Ideal Continuous Tracking*: continuous monitoring of the alumina concentration to manage a binary alumina feeding policy and continuous tracking of the cell pseudo resistance to manage the ACD.

- *Pechiney Continuous Tracking*: continuous tracking of the cell pseudo resistance to manage a fixed binary alumina feeding policy mixed with resistance control [11].
- *Demand Continuous Tracking*: continuous tracking of the cell pseudo resistance to manage an adjustable tertiary alumina feeding policy mixed with resistance control [12].

Validation Exercise

It is clear from the previous discussion that modeling the behavior of a reduction cell is fairly complex. One is left with the question whether it is possible to adequately simulate the process. Hence, thorough validation of the program is critical.

Two levels of validation can be identified. The first ensure that the program performs as it should, i.e. the input data is properly stored and accessed, the equations in the submodels are coded correctly, the control logic and the interaction between events and cell states is properly represented, etc. This level of validation was achieved by running a number of examples designed to test various combinations of features as part of the software quality assurance (QA) program.

The second level looks at a particular cell design and ensures that the program can adequately predict the measured behavior. Successful validation depends on two factors: accurate representation of the cell characteristics; and accurate measurements. The cell characteristics include the geometry, material properties, operational procedures and so forth. It also includes proper selection of the equations that characterize the process.

Aratu 1984 Measurement Campaign

Satisfied with the results of the QA program, the next step was to validate a model of an operating cell. The Aratu smelter, owned by Alcan Brazil, had characterized experimentally the dynamic behavior of their V.S. pots in the early days of the smelter. This data has been used to validate a model of the operating cell.

The extensive measurement campaign that was carried out at the time consisted of measuring several data from two pots. These included the bath temperature, the concentration of alumina dissolved in the bath and the concentration of excess AlF_3 in the bath. Measurements were taken every hour for a period of 24 hours. The data is presented in figures 1 and 2.

At the time of the measurements, the typical operational characteristics of the Aratu V.S. potline were:

Amperage	120 kA
Cell voltage	4.2 V
Current efficiency	89%
ACD	4.3 cm
Concentration of excess AlF_3	8%
Average bath temperature	980 °C
Bath level	19 cm
Metal level after tapping	33 cm
Metal tapped each day	860 kg
Alumina feed per break	125 kg
Break frequency	2 hrs 40 min
Alumina feed per anode effect	250 kg
Average anode effect frequency	2 per day
Net anode consumption	530 kg C/t Al

As can be seen in figures 1 and 2, the data obtained is very consistent, showing that the process was well under control during the measurements and that the experimental sampling errors were minimized. Furthermore, the measured behavior compares favorably with the above operational characteristics with the exception of the anode effect frequency. Pot A had 3 anode effects that day while pot B had 4. This discrepancy indicates that the target average break feed of 125 kg was not achieved consistently (other less probable reasons could be poor alumina dissolution or higher current efficiency).

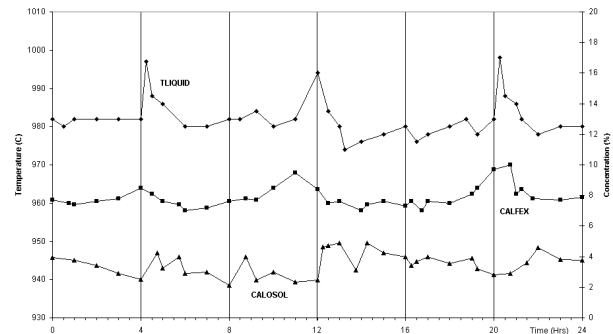


Figure 1: Measurements from Pot A. TLIQUID: bath temperature; CALOSOL: concentration of dissolved Al_2O_3 ; CALFEX: concentration of excess AlF_3 .

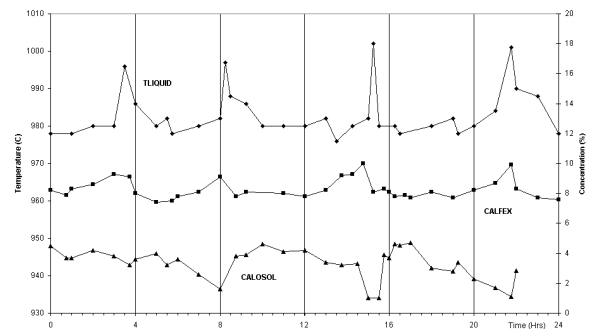


Figure 2: Measurements from Pot B. TLIQUID: bath temperature; CALOSOL: concentration of dissolved Al_2O_3 ; CALFEX: concentration of excess AlF_3 .

Model Results

Data obtained from a thermo-electrical blitz campaign carried out when the measurements were taken along with the cell geometry and operational characteristics were used to define a model of the Aratu pot¹. Published equations were used in the submodels to characterize the process behavior.

The first step in processing the model was to obtain a steady state solution to start the transient run. It was relatively simple to fine tune the model to closely reproduce the target cell characteristics noted above. Input values (such as the operating temperature, bath chemistry, anode/cathode heat dissipation, etc.) were adjusted within the measured range. Calculated values such as the ACD, current efficiency, cell voltage, etc. are shown in Table II. They compare favorably with the target values.

¹Close to 60 items of data are required to characterize the cell. This is facilitated by providing default values where appropriate.

Table II: Calculated Steady State Solution

ACD (cm)	4.299
Current efficiency (%)	88.960
Cell voltage (V)	4.210
Superheat (°C)	5.580
Ledge thickness, adjacent to bath (cm)	12.299
Ledge thickness, adjacent to metal (cm)	29.998
Alumina feeding rate (kg/hr)	67.709
Aluminum fluoride feeding rate (kg/hr)	0.263
Target cell resistance (??)	21.336

Starting from the steady state solution and using the typical operational characteristics, the transient solution was obtained. A two minute time step was selected resulting in 5040 time steps required to simulate a seven day period. It took 40 seconds on a 486 DX2 PC to calculate the solution.

The time history of the measured variables is reported in figure 3. We can see that the predicted dynamic behavior is characterized by a 12 hour anode effect cycle which is a natural outcome of the selected feeding strategy. Additional information was available from the solution as described below.

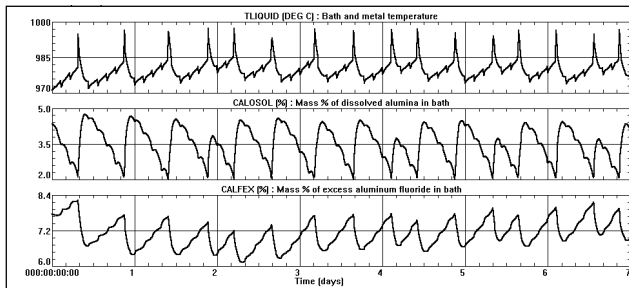


Figure 3: Calculated bath temperature (TLIQUID), concentration of dissolved Al_2O_3 (CALOSOL) and concentration of excess AlF_3 (CALFEX).

Comparison of the Measured and Calculated Response

Having presented the measured and calculated results, we can compare more closely the two dynamic responses. Given the randomness of the anode effect occurrences observed in the measured data, we will restrict the comparison to one set of measurements (Pot A) for a 24 hour simulation period.

Figure 4 clearly demonstrates that the model reproduces every feature of the measured dynamic evolution of the bath temperature, namely

- the temperature drop at each crust break;
- the slow temperature increase between crust breaks;
- the rapid temperature increase during an anode effect; and
- the rapid temperature drop after an anode effect.

We can deduce the same conclusion from figure 5 which compares the time history of the alumina concentration. Again the model reproduces every feature of the dynamic evolution, namely

- the small humps between crust breaks;
- the global decrease due to the insufficient feeding; and
- the fast 2% increase when the anode effect occurs and is killed.

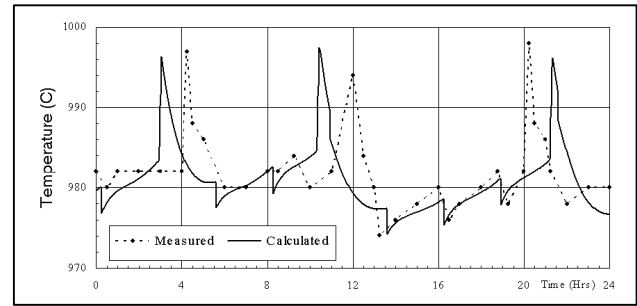


Figure 4: Measured vs. calculated bath temperature.

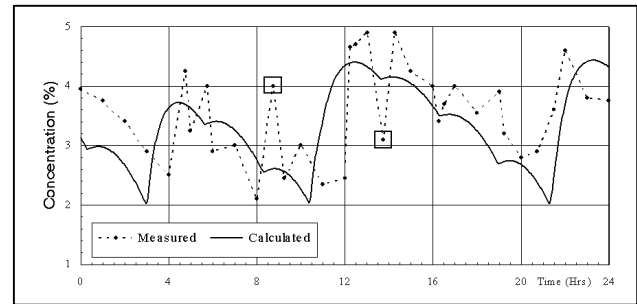


Figure 5: Measured vs. calculated alumina concentration.

Note that there seem to be two points in the measured data (figure 5) which are not consistent with the expected behavior of the cell. These are close to the 9 and 14 hour mark and should be discarded.

The comparison of the % excess AlF_3 dynamic evolution is presented in figure 6. Two observations are noted:

- The fast decrease in concentration that corresponds to the fast melting rate of the ledge is well reproduced.
- The model failed to pick up the fast increase in concentration that occurs before an anode effect. Rather, it predicts a slow increase that corresponds to the slow formation of the ledge between anode effects.

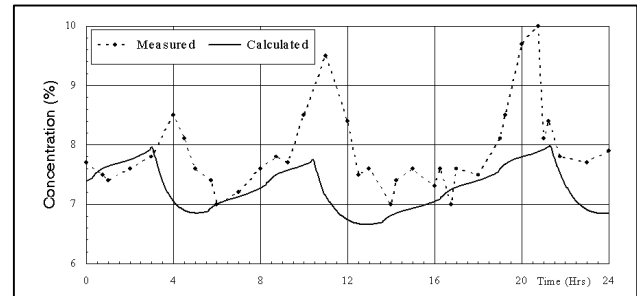


Figure 6: Measured vs. calculated % excess AlF_3 .

It is clear that even if the model shows the right trend, it underestimates the amplitude of the % excess AlF_3 fluctuation. We attribute the change in concentration before the anode effect primarily to the depletion of cryolite due to the absorption by the crust. This would explain the discrepancy between the model and measured data since the program does not account for the effect of the crust formation and its interaction with the bath.

The above results demonstrate that the program has successfully reproduced the complex dynamic behavior measured in the Aratu cell. This indicates that the published behavioral models used in the program are fairly accurate and that when grouped together they generate a good approximation of the process behavior.

Additional Information Available from the Model

The good agreement between the model and the measurements provides us with the confidence to investigate the evolution of other variables that were not measured. For example, we can look at the dynamic evolution of the superheat, the fluoride evaporation rate and the average ledge thickness adjacent to the bath to pick a few. The time history of the above is shown in figure 7.

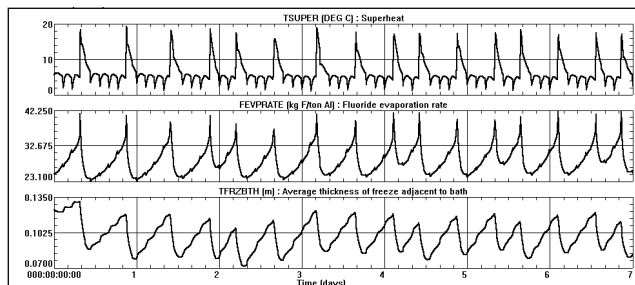


Figure 7: Calculated superheat (TSUPER), fluoride evaporation rate (FEVPRATE) and average ledge thickness adjacent to the bath (TFRZBTH).

The dynamic evolution of these variables is close to impossible to measure experimentally. However, the simulation provides the time history to help understand the complex interaction between different variables. For instance, the similarity between figures 3 and 7 demonstrates that the evolution of the % excess AlF_3 is driven by the ledge thickness evolution.

Continuous Potline Improvement Project

What is even more useful to the process engineer is the availability of a validated model of the potroom to help investigate "what if" scenarios.

To illustrate potential applications of the model, let us investigate the impact of reducing the number of anode effects by changing the amount of alumina fed in a scheduled break from 125 to 185 kg. In particular, we are interested in the changes to the bath temperature and the alumina concentration.

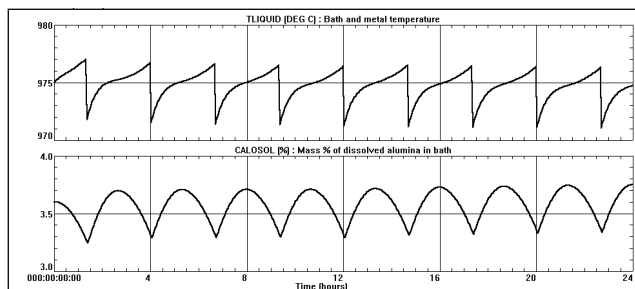


Figure 8: Time history of the bath temperature (TLIQUID) and the alumina concentration (CALOSOL) using a one day simulation with 185 kg alumina fed per break.

A one day simulation seems to indicate that the pot will operate without problems (see figure 8) while a longer simulation time reveals that this change on its own would quickly cool down and sludge the pot (see figure 9). The temperature drop is obviously a consequence of the imbalance between the heat loss and the new internal heat.

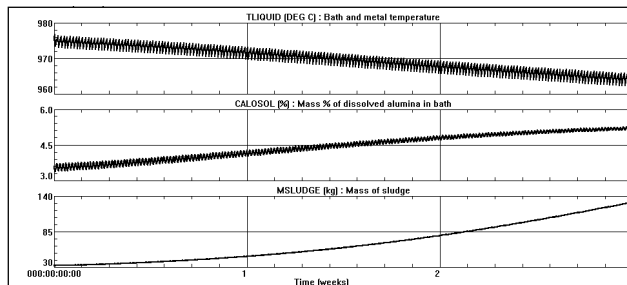


Figure 9: Time history of the bath temperature (TLIQUID), the alumina concentration (CALOSOL) and the mass of sludge (MSLUDGE) using a three week simulation with 185 kg alumina fed per break.

This imbalance is a result of the uncompensated loss of the heat produced during an anode effect. The gradual increase in the alumina concentration in the bath is an indication that the pot is gradually sludging. This is confirmed by looking at the evolution of the sludge shown in figure 9.

The next logical step would be to use the program to evaluate the following possibilities:

1. Adjusting the heat balance requirement by
 - defining new operating conditions that will maintain a steady operating temperature (i.e. lower metal level, adjust the target cell pseudo-resistance, etc.); or
 - revising the cathode lining design based on the new requirement for cathode heat dissipation.
2. Developing a new operating procedure to avoid sludging the pot while still reducing significantly the anode effect frequency (for example establish rules to skip a break based on the behavior of the cell pseudo-resistance slope).

Conclusions

A computer program has been developed to simulate the dynamic behavior of a reduction cell. The program has sufficient capabilities to model the process as well as the control logic employed in most cell operations.

The program was successfully used to simulate the behavior of the Aratu cell. Comparison of the calculated response with measured data provided the confidence to investigate several operational procedures that could improve pot performance.

References

- [1] X. Wang, R.D. Peterson, and A.T. Tabereaux, "A Multiple Regression Equation for the Electrical Conductivity of Cryolytic Melts", *Light Metals*, (1993), 247-255.
- [2] G. Choudhary, "Electrical Conductivity for the Electrolytes of Aluminum Extraction Cell", *J. Electrochem. Soc.*, 120(3) (1973), 381-383.

- [3] P.A. Solli, T. Haarberg, T. Eggen, E. Skybakmoen and A. Sterten, "A Laboratory Study of Current Efficiency in Cryolitic Melts", Light Metals, (1994), 195-203.
- [4] E.W. Dewing, "The Chemistry of the Alumina Reduction Cells", Can. Met. Quart., 13(4) (1974), 607-617.
- [5] A. Solheim, S. Rolseth, E. Skybakmoen and L. Steen, "Liquidus Temperature and Alumina Solubility in the System $\text{Na}_3\text{AlF}_6\text{-AlF}_3\text{-LiF-CaF}_2\text{-MgF}_2$ " Light Metals, (1995), 451-460.
- [6] W. Haupin, "Cell Voltage Components", CMP/PCPE Course on Aluminum Electrolysis, (1994).
- [7] W. Haupin, "Heat Balance and Energy Consumption", CMP/PCPE Course on Aluminum Electrolysis, (1994).
- [8] J. Chen, W. Chuck, S. Thomson, B. Welch, and M. Taylor, "A Study of Cell Ledge Heat Transfer using an Analogue IceWater Models", Light Metals, (1994), 285-293.
- [9] W. Haupin, and H. Kvande, "Mathematical Model of Fluoride Evolution from Hall-Héroult Cells", Light Metals, (1993), 257-263.
- [10] L. Tikasz, R.T. Bui, and V. Potocnik, "Aluminium Electrolytic Cells: A Computer Simulator for Training and Supervisions", Engineering with Computer, (10)(1994), 12-21.
- [11] Y. Macaudiere, "Recent Advances in Process Control of the Potline", Light Metals, (1988), 607-612.
- [12] K. R. Robilliard and B. Rolofs, "A Demand Feed Strategy for Aluminum Electrolysis Cells", Light Metals, (1989), 269-273.